Research Article

Microwave Radiation Induced Human iPSC Derived Cardiomyo-cytes Injury

Liang Yue[1#]; Jing Zhang[2#]; Zhi-Min Yun[1]; Peng-Fei Zhong[1,4]; Rui-Lin Ma[1,3]; Xin-Ping Xu[2]; Hong-Tu Cui[1]; Bin-Wei Yao[2]; Lei-Ming Fang[1]; Qi Liu[1]; Cheng-Jun Wu[3]; Rui-Yun Peng[2*]; Ying-Xia Tan[1*]

[1]Institute of Health Service and Transfusion Medicine, Academy of Military Medical Sciences, Academy of Military Sciences, Beijing, China

[2]Beijing Institute of Radiation Medicine, Academy of Military Medical Sciences, Academy of Military Sciences, Beijing, China

[3]School of BME, Faculty of Medicine, Dalian University of Technology, Dalian, China

[4]Graduate School, Hebei North University, Zhangjiakou, Hebei Province, China

*Corresponding author: Ying-Xia Tan

Institute of Health Service and Transfusion Medicine, Academy of Military Medical Sciences, Academy of Military Sciences, Beijing, China.

Rui-Yun Peng, Beijing Institute of Radiation Medicine, Academy of Military Medical Sciences, Academy of Military Sciences, Beijing, China.

Email: ruiyunpeng18@126.com; tanhu333@126.com

[#]These authors have contributed equally to this article.

Abstract

Electromagnetic waves are recognized as the third major source of pollution, which can damage to the heart. However, due to the limitation of human subjects in research, it is difficult to extrapolate the biological effects of electromagnetic waves directly from animals to humans. In this study, human induced pluripotent stem cell-derived cardiomyocytes (hiPSC-CMs) were used to explore the effect of microwave radiation on human heart injury. Human iPSC-CMs were radiated with a single irradiation dose of 30W/Kg for 30 min. After radiation, the content of Reactive Oxygen Species (ROS) in hiPSC-CMs increased significantly, and the Mito-tracker and mitochondrial membrane potential decreased synchronously. Seahorse assay found that the mitochondrial functions in cardiomyocytes were weakened after being exposed irradiation. The electrophysiological functions of hiPSC-CMs were significantly abnormal, with increased proportions of late apoptosis and decreased proportions of viable cells. In addition, the secretion of 10 pro-inflammatory cytokines/chemokines was increased in hiPSC-CMs after radiation. An effector model of microwave irradiation-induced cardiac injury was established using hiPSC-CMs in this study. Based on the fully observation of the structure and functions of iPSC-CMs after radiation, it was speculated that mitochondrial damage might be the dominant cause of delayed intracellular energy transfer, which was synchronously manifested as abnormal electrophysiological functions. The findings of this study provide valuable data for the clinical transformation of basic experimental research, and the damage mechanism will be explored in the future in order to provide effective assistance to the occupational practitioners.

Keywords: Microwave; hiPSC-CMs; Mitochondria; Cytokines; Apoptosis

Introduction

As an important member of the electromagnetic wave family, microwave is widely used in people's lives and work [1,2]. While it brings convenience to people's lives, it also causes certain health problems [3], such as insomnia, chest pain, and other symptoms. Studies have confirmed that microwave radiation has multi-system and multi-target effects on living organisms [4], of which heart is a particularly important target [5]. The cardiovascular system is one of the target systems that is sensitive to microwave radiation [6]. Microwave radiation can disrupt energy metabolism in cardiomyocytes, causing metabolic dysfunction and even apoptosis, resulting in structural and functional abnormalities in the heart [7]. The heart is the crucial organ in the circulatory system that ensures the blood supply to the organs of various organs of the body is maintained [8].

Epidemiological investigations have demonstrated that long-term exposure to low doses of microwave radiation can cause discomfort in the heart area of radiated individuals, and severe cases may exhibit symptoms such as chest tightness and precordial pain. Due to the influence on autonomic neuromodulation, irradiated individual mostly experience bradycardia, and a few with tachycardia [9,10]. Long-term, repeated exposure to microwave radiation with a power density greater than 100mW/cm 2 can lead to organic changes in the rat human cardiovascular system, such as palpitations, chest tightness, precordial pain, hypotension, slow heart rate, atrial and ventricular conduction delays, and ECG waveform changes [11]. At present, Wistar rats are commonly used animals for establishing models, and primary rat cardiomyocytes and murine H9C2 cell lines are frequently

used cells in research on cardiac damage caused by microwave radiation. However, there is a big gap between these animal models and the human body, and a lack of objective evaluation indicators that can be converted for use in humans [12].

The depolarization process of human cardiomyocytes differs significantly from that of rodents. For example, under normal physiological conditions, the human heart rate is about 60-90 beats per minute, while the heart rates of rats and mice are 300-400 and 500-700 beats per minute, respectively. Consequently, there are great differences in comparability between different species and between the same species.

The bottleneck problem restricts the transformation of experimental results in this field. At present, iPSC-CMs have been successfully applied in clinical patients with heart failure and can characterize the complex physiological functions of human cardiomyocytes in vitro [13].

In this study, iPSC-CMs were taken as the modeling subject to study the effects of microwave radiation. The S-band was chosen as the simulated source of microwave radiation which was demonstrated in animal studies. And changes in the structure and function of iPSC-CMs were monitored. The purpose of this study was to explore new effect indicators and possible damage mechanisms, in order to provide a better fundamental work for the related research on protection and damage mechanisms [14].

Materials and Methods

hPSC Differentiation into Cardiomyocytes

Cardiomyocyte differentiation was performed on hiPSCs-B1 (blood-derived iPSCs, CA4025106, Cellapy). B1 hiPSC line (CA4025106, Cellapy) was cultured in mTeSR medium (Stemcell, 05850) and incubated at 37°C with 5% CO2. In brief, differentiation medium 1 consisted of RPMI 1640 (Gibco, 1744361) and B-27 (Gibco, A1895601), with extra CHIR-99021 (6 μM, Selleckchem, S2924) on day 0 and day 1 and IWR-1 (5 μM, Sigma, 10161) on day 4 and day 5. The medium was replaced with fresh differentiation medium 2 consisting of RPMI 1640 (Gibco, 1744361), B-27 (Gibco, A1895601), and 2% FBS on day 8.

Immunofluorescence Staining

The hiPSC-CMs were fixed in 4% PFA for 20 min and permeabilized with 0.1% Triton-X 100 for 5 min. The cells were incubated with the following primary antibodies overnight at 4°C: Troponin T 1:100, α- actinin 1:50. Then cells were washed with PBS and incubated with Alexa-conjugated secondary antibodies. Nuclei were stained with DAPI (Life Technologies, P36931). All images were acquired using a Nikon A1 confocal microscope.

Microwave Radiation

The hiPSC-CMs were divided into group C (the normal control group) and group R (the S-band radiation group). The dose was 30W/Kg for a single irradiation of 30min.

Transmission Electron Microscopy

At 24 h after radiation, hiPSC-CMs were scraped off with soft silicone sheets and centrifuged at 10,000 rpm for 10 min. The supernatant was removed; specimens were fixed in 2.5% glutaraldehyde fixation solution for 2h and 1% osmic acid fixation solution for 1h. Specimens were dehydrated in gradient ethanol and embedded in Epon-812 resin. Ultra-thin sections with a thickness of 70 nm were made and stained in uranium acetate and lead nitrate. All images were acquired using a transmission electron microscope (Hi-tachi).

Electrophysiological Detections

At 36 h after radiation, the field potential (beat period, FPD, FPDc and spike amplitude) and cell contractility (beat amplitude, excitation-contraction delay and mean beat width) of hiPSC-CMs were measured using a microelectrode application platform (Axion BioSystems).

Mito-Tracker Green Staining

The hiPSC-CMs were incubated with staining working solution containing 200 nM Mito-Tracker green (M46750, Invitrogen) for 45 min at 37°C. (1) After incubation with 1:1000 dilution of Hoechst 33342 for 10 min, images were acquired using a fluorescence microscope. (2) hiPSC-CMs were digested after staining, and fluorescence intensity was detected by flow cytometry. The average fluorescence intensity was calculated and analyzed using FlowJo software.

Detection of Mitochondrial Membrane Potential

The hiPSC-CMs were incubated with staining working solution containing 150nM TMRE (HY-D0985A, MCE) at room temperature in the dark for 10 min. (1) After incubation with 1:1000 dilution of Hoechst 33342 for 10 min, images were acquired using a fluorescence microscope. (2) hiPSC-CMs were digested after staining, and fluorescence intensity was detected by flow cytometry. The average fluorescence intensity was calculated and analyzed using FlowJo software.

Detection of Reactive Oxygen Species

The hiPSC-CMs were incubated with a staining working solution containing 5μM DCFH-DA (HY-D0940, MCE) at 37°C for 45 min. (1) After incubation with 1:1000 dilution of Hoechst 33342 for 10 min, images were acquired using a fluorescence microscope. (2) hiPSC-CMs were digested after staining, and fluorescence intensity was detected by flow cytometry. The average fluorescence intensity was calculated and analyzed using FlowJo software.

Seahorse Assay

The hiPSC-CMs (10^5 cells/well) were plated on an XF24 cell culture microplate coated with poly-D lysine (50 μg/mL). After being cultured at 37°C for two days (90% confluency of cells was reached), hiPSC-CMs were radiated and Seahorse assay was performed 24 h after irradiation. Experiments were done in XF assay medium that contained 25 mM glucose, 2 mM L-glutamine and 1 mM Na pyruvate and analyzed using a Seahorse XFe24 Extracellular Flux Analyzers (Agilent Technologies). When indicated, the following were injected: oligomycin (1 μM), carbonyl cyanide 4-(trifluoromethoxy) phenylhydrazone (FCCP; 1 μM), rotenone (0.5 μM) and antimycin A (0.5 μM), glucose (10mM), oligomycin (1μM) and 2-Deoxy-D-glucose (2-DG; 50mM). Basal OCR and ECAR reports were generated by Wave Desktop software (Agilent Technologies).

Cytokines and Chemokine Assays

The supernatant of hiPSC-CM cultures was collected at 24 h after radiation to detect cytokines using Bio-Rad Bio-Plex Pro human cytokine 48-Plex assay and chemokine panel 40-plex kits (Bio-Rad, Hercules, CA, USA) according to the manufacturer's instructions. A total of 69 cytokines and chemokines were detected. Each sample was incubated in 96-well plates embedded

with microbeads for 30 min and then incubated with detection antibody for 30 min. Furthermore, streptavidin-PE was filled in each well for 10 min, and values were read on Bio-Plex MAG-PIX System (Bio-Rad, Hercules, CA, USA). The experiments were performed by Wayen Biotechnologies (Shanghai, China).

Apoptosis Assay

Apoptosis was detected using annexin V-FITC apoptosis detection kits (APOAF, Sigma) at 24 h after irradiation. The hiPSC-CMs were washed twice with DPBS and resuspended in a binding buffer at a concentration of 10^6 cells/mL. 5 µL of annexin V-FITC conjugate and 10 µL of propidium iodide solution were added to each cell suspension and incubated for 10 min at room temperature in the dark. The fluorescence intensity was measured immediately using a flow cytometer. The hiPSC-CMs in the early stages of the apoptotic process were stained with annexin V-FITC conjugate only. Viable hiPSC-CMs were not stained with either propidium iodide solution or annexin V-FITC conjugate. Necrotic hiPSC-CMs were stained with both propidium iodide solution and annexin V-FITC conjugate.

Statistical Analyses

The data in this paper were expressed as mean ± Standard Deviation (SD), the student's t tests were used to analyze the difference between two groups, and all statistical analyses were two-tailed. The acceptable level of significance for all tests was $P<0.05$. The marker *represents $P<0.05$, **represents $P<0.01$ and ***represents $P<0.001$.
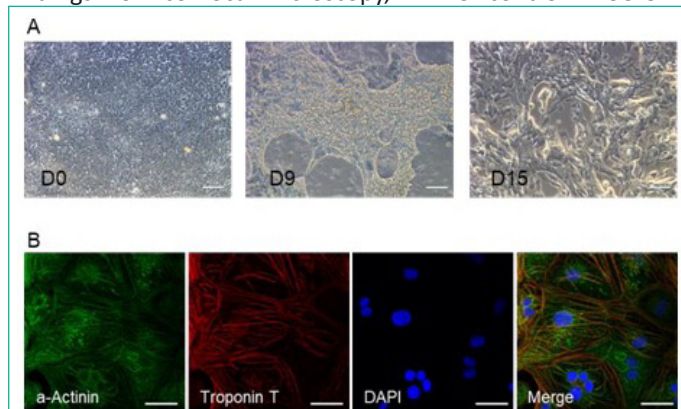
Results

Human Induced Pluripotent Stem Cells-Derived Cardiomyocytes

A small molecule-based monolayer differentiation protocol was adapted for cardiomyocyte differentiation in vitro using blood derived iPSCs (hiPSCs-B1). Spontaneously contracting Cardiomyocytes (CMs) were observed under light microscopy at days 8-10 after initiation of differentiation (Figure 1A). After 15 days in culture, hiPSC-CMs were immunostained illustrating that cells robustly expressed cardiac Troponin T and cardiac contractile proteins α-actinin (Figure 1B), showing successful differentiation.

Ultrastructural Damage Caused by Microwave Radiation

The ultrastructural elements were further analyzed by Transmission Electron Microscopy (TEM). Consistent with the findings from confocal microscopy, TEM of control hiPSC-CMs showed that myofibrils were arranged neatly in the cytoplasm, with clear light-dark bands (Figure 2A), and that intracellular mitochondria were of regular shape and possessed dense cristae (Figure 2B). These findings indicate an ultrastructural maturation of hiPSC-CMs. At 24 hours post-irradiation, a large number of vacuolated and swollen mitochondria appeared in cardiomyocytes, and mitochondrial cristae were reduced or even disappeared (Figure 2B). This resulted in less dense myofibrils and shortened Z-lines (Figure 2A), indicating that radiation caused significant damage to myofibrils and mitochondria in cardiomyocytes. The damage to myofibrils and mitochondria caused by radiation can trigger changes in the contractility of cardiomyocytes and even impairs energy transfer.

Electrophysiological Functions of hiPSC-CMs after Microwave Radiation

Electrophysiological assays were performed to investigate the effect of microwave radiation on cardiomyocyte contractility. The results showed that compared with the control, microwave radiation caused a significant reduction in the field potential and contractility (Figures 3A and 3B) ($P<0.01$). In addition, the beat amplitude was significantly ($P<0.01$) reduced and the mean beat width was also shortened significantly ($P<0.01$) shortened at 36 h post-irradiation (Figure 3C). These results suggest that microwave radiation has a negative effect on cardiomyocyte contractility. There were no differences in beat period and excitation-contraction delay between the control and radiation groups (Figure 3C). The results showed that electrophysiological parameters related to cardiomyocyte contractility were significantly altered after exposure to microwave radiation, as evidenced by decreases in both beat amplitude and contraction time. These changes may be related to previously detect structural changes such as the loose and disordered arrangement of myofibrils caused by radiation.
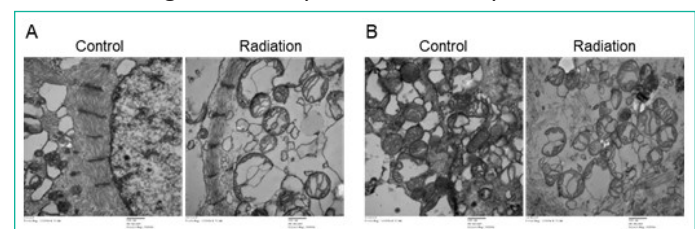
Figure 2: Cellular ultrastructure of hiPSC-CMs observed by transmission electron microscope. (A) Myofil-aments are present in hiPSC-CMs at 24 hours post-radiation. (B) Mitochondrial structure in hiPSC-CMs were destroyed at 24 hours post-radiation. Scale bar=500nm.
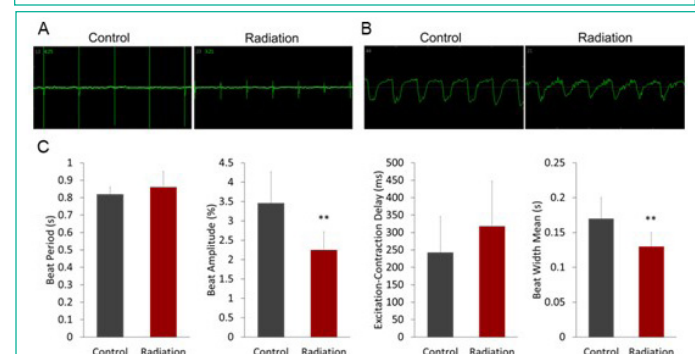
Figure 3: Electrophysiological functions of hiPSC-CMs are detected after microwave radiation. (A) The field potential of hiPSC-CMs at 36h post-radiation. (B) The contractility of hiPSC-CMs at 36h post-radiation. (C) Histograms of field potential (beat period) and contractility (beat amplitude, excitation-contraction delay, and mean beat width) parameters of hiPSC-CMS detected 36 h after radiation. **$P<0.01$ estimated by Student's t test.

Figure 1: Identification of cardiomyocyte differentiation. (A) Representative images at D0, D9, and D15 during cardiomyocytes differentiation. (B) Immunofluorescence staining of cardiac troponin T and a- actinin in hiPSC-CMs. Scale bar=100 µm.

Microwave Radiation Induces Mitochondrial Dysfunction in hiPSC-CMs

Mitochondria are rich in cardiomyocytes. It was observed by electron microscopy that there was obvious acuolization of mitochondria after radiation. Then whether microwave radiation affected mitochondrial function was further investigated. The level of ROS in cardiomyocytes was significantly increased (*P*<0.01) at 24h post-radiation (Figure 4A). Meanwhile, the mitochondrial mass and Mitochondrial Membrane Potential (MMP) were significantly decreased (*P*<0.01 and *P*<0.05) in cardiomyocytes (Figures 4B & 4C). The mitochondrial structure in cardiomyocytes was observed by a TEM at 24h post-radiation, and large number of vacuolated and swollen mitochondria appeared in cardiomyocytes after radiation. The internal cristae dissolved or even disappeared, consistent with the above findings. These results suggested that microwave radiation might damage the mitochondrial structure of cardiomyocytes, causing mitochondrial dysfunction and intracellular ROS accumulation, which could lead to increased oxidative damage to intracellular DNA and ultimately induce cell apoptosis.

Cellular Respiration Detected by Seahorse Assay

Mitochondrial functions were detected by seahorse assay at 24 h after radiation. It was found that the mitochondrial functions in cardiomyocytes were weakened after being exposed irradiation. The key parameters such as basal respiration, maximal respiration, ATP production, and spare respiratory capacity decreased significantly (*P*<0.01, *P*<0.05, *P*<0.01, and *P*<0.05, respectively) after radiation. There were no significant differences in proton leak (*P*=0.9439), non-mitochondrial oxygen consumption (*P*=0.1862), coupling efficiency (*P*=0.09841), and the proportion of spare respiratory capacity to basal respiration

(*P*=0.5774) between the control and radiation groups (Figure 5A). In addition, glycolytic capacity was reduced significantly in cardiomyocytes after radiation (*P*<0.05), however, the levels of glycolysis remained unchanged (*P*=0.0850). There was no significant difference between the control and radiation groups in glycolytic reserve (*P*=0.4365) and the proportion of glycolytic reserve to the basal value (*P*=0.8765). Non-glycolytic acidification decreased significantly (*P*<0.01) (Figure 5B). Structural changes are the material basis for the functional changes. Therefore, the impairment of mitochondrial structure in cardiomyocytes by radiation is associated with dysfunction of energy transfer, as evidenced from the synchronization of the timeline.

### The Changes of Cytokines Caused by Radiation

Cytokines and chemokines are essential cellular modulators of various physiological and pathological activities. To determine whether irradiation contributes to innate immune response, cell culture supernatants were collected after radiation for cytokine detection using the Bio-Rad Bio-Plex Pro human cytokine 48-Plex assay and chemokine panel 40-plex kits. The levels of cytokines and chemokines expressed by the radiated cardiomyocytes were found to be significantly different from those in the control group. The data showed that 24h post-irradiation, the secretion of cytokines was significantly increased compared to the control group. For each detected cytokine, 10 of the total 69 cytokines, TNF-α (*P*<0.001), IL-1α, MIP-1α, CXCL12, IL-5 (*P*<0.01), MCP-2, CXCL13, IP-10, IL-16 and IL-10 (*P*<0.05), were significantly increased in the cell supernatant at 24h post-irradiation (Figure 6), indicating that microwave radiation caused inflammatory responses in cardiomyocytes.

### Microwave Radiation Induced Cardiomyocyte Apoptosis

Based on the above results, we speculate that microwave radiation may cause cardiomyocyte apoptosis. To confirm this, flow cytometry was used to detect cardiomyocyte apoptosis after radiation. The results showed that the number of alive cells decreased significantly (*P*<0.05) and the number of late apoptotic cells increased significantly (*P*<0.01) after radiation (Figure 7). However, there was no significant difference between the
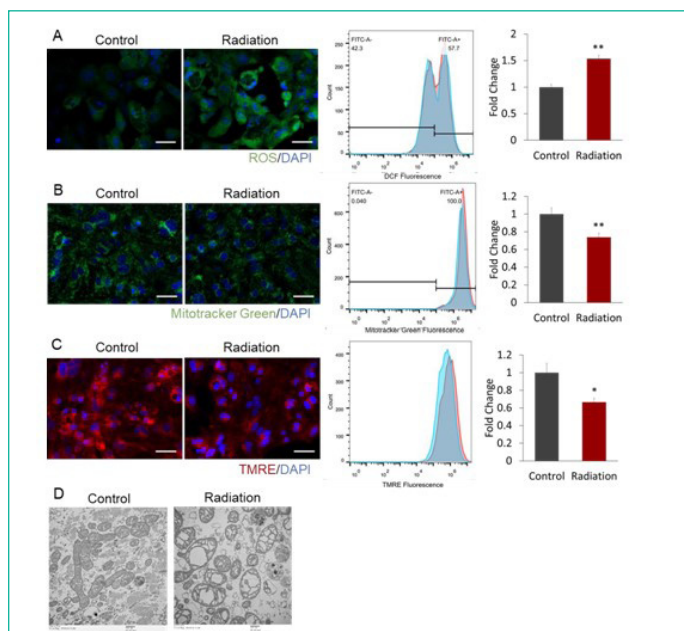

Figure 4: Microwave radiation induces mitochondrial dysfunction in hiPSC-CMs. (A) The Reactive Oxygen Species (ROS) in hiPSC-CMs were measured at 24h after radiation using DCFH-DA. (B) The mitochondrial mass in hiPSC-CMs was detected at 24h after radiation using Mito-tracker green. (C) The Mitochondrial Membrane Potential (MMP) in hiPSC-CMs was tested at 24h post-irradiation using Tetramethylrhodamine Methyl Ester (TMRE). The representative images (left), representative histogram (middle) and quantification of the mean fluorescence intensity (right) are presented for (A) to (C), Scale bar=100 µm. *P*<0.05 and **P*<0.01 were estimated by Student's t test. (D) Mitochondrial structure in hiPSC-CMs at 24 hours post-radiation was detected by TEM. Scale bar=500nm.
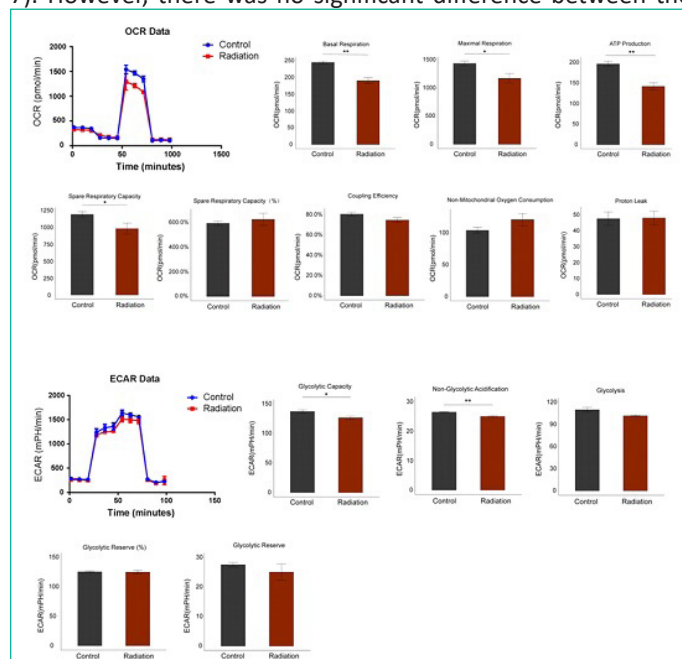
Figure 5: Microwave radiation induces mitochondrial respiratory disorders in hiPSC-CMs. (A) The mito chondrial function and (B) the glycolytic capacity of hiPSC-CMs were detected at 24h after radiation using Seahorse assay.
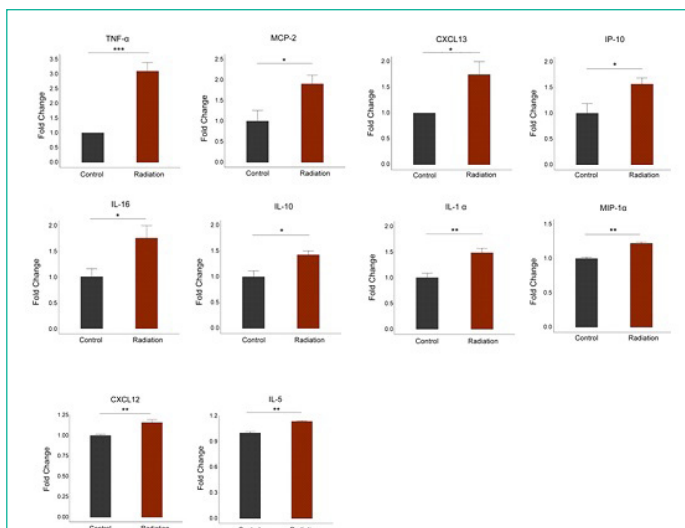
Figure 6: Elevated inflammatory factors in hiPSC-CMs after radiation. Radiation exposure leads to increased production of pro-inflammatory cytokines in hiPSC-CMs.
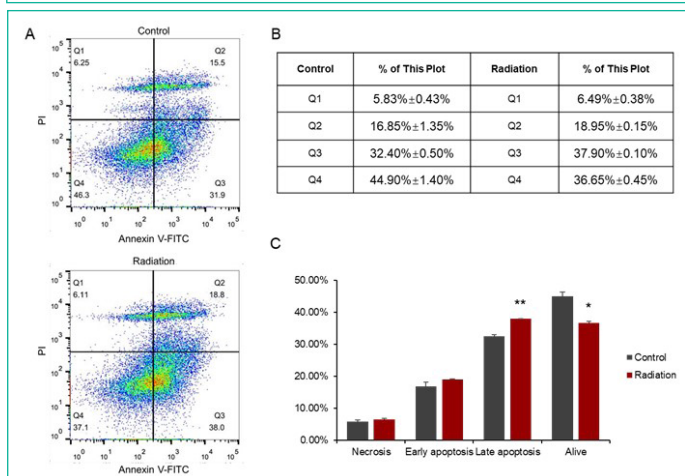
Figure 7: Cardiomyocyte apoptosis induced by radiation. (A) Distribution of cells in the 4 quadrants in the control and radiation groups detected by flow cytometry. (B) the values of flow cytometry. Figure C is a histogram based on Figure B.

control group and the radiation group in the early apoptotic cells and necrotic cells (Figure 7). The above results indicate that microwave radiation can cause cardiomyocyte apoptosis.

Discussion

As the third major source of pollution after water and air, electromagnetic irradiation has been paid more and more attention in the research of environmental toxicology [15]. As one of its sensitive target organs, the heart has also attracted much attention in recent research. However, one of the major obstacles to the advancement of this area is how to transform the findings from numerous animal studies into humans applications [16]. In this study, the damage effect in human iPSC-CMs was evaluated, and conducted targeted observations were conducted on the structure and function of hiPSC-CMs to gain a better understanding of the health and safety of irradiation related practitioners.

Microwaves are very important member of the electromagnetic wave family. They are widely used in many emerging technological fields, such as communications, medical treatment, and the military. They are also the most studied type of electromagnetic irradiation in the field of biology [2]. This study found that 24 hours after undergoing S-band irradiation, hiPSC-CMs present structural changes mainly consisting of loosely arranged myofibrils, sarcomere widening, and mitochondrial vac-

uolization. These changes potentially impact the function of the human heart. Since the beat frequency of hiPSC-CMs is similar to that of the human heart, electrophysiological functions were taken as the important indicators for real-time evaluation after microwave radiation. Results showed that beat amplitude and mean beat width decreased significantly in the radiation group. Electrophysiological parameters related to the contractility of cardiomyocytes changed significantly after radiation. Beat amplitude and contraction time both decreased, which may be due to structural changes in myofibrils, such as loose and disordered arrangements caused by radiation.

In addition, structural damage is the important material basis for functional changes [14,17]. In this study, mitochondrial function was detected to deeply explore the consequences of structural damage. After radiation, ROS content in cardiomyocytes increased significantly, mitochondrial mass and mitochondrial membrane potential decreased. When observing mitochondrial structure in cardiomyocytes by transmission electron microscope, it was found that a large number of vacuolated and swollen mitochondria appeared in cardiomyocytes after radiation, with internal cristae dissolved or even disappeared. The structural and functional results indicated that there was mitochondrial dysfunction in cardiomyocytes, which was logically consistent with the results of the Seahorse assay and electrophysiological test.

Although cardiac structural and functional damage by microwaves radiation was investigated. However, it is important to explore dynamic changes of biomarkers or cytokines that could be more easily connected to clinical applications [17,19]. It was reported that the levels of inflammatory factors in the supernatant of human cardiomyocyte cultures changed after radiation.

In this study, Bio-Plex assay showed that the expression levels of 10 pro-inflammatory cytokines/chemo-kines (MCP-2, CXCL13, IP-10, IL-16, IL-10 (P<0.05), IL1-α, MIP-1-α, CXCL12, IL-5 (P<0.01), TNF-α (P<0.001)) increased significantly in hiPSC-CMs after radiation. Among these factors, TNF-α increased most significantly. TNF-α, also known as a pro-inflammatory cytokine, is considered a factor at the center of inflammatory cascade reactions. When an inflammatory response occurs, the expression and release of TNF-α increase, and a series of cascade reactions are triggered, leading to the upregulation of the expression of multiple inflammatory factors [19,20]. One study showed that mitochondria not only underwent numerous changes when the body was stimulated to trigger an inflammatory response, but also played a key regulatory role in the inflammatory response [21]. Under the stimulation of pro-inflammatory factors, ROS and inflammatory mediators released from cells can damage mitochondria structurally and functionally. Damage to mitochondrial functions, such as the release of ROS [22-25] and mtDNA [26], and the imbalance of mitochondrial dynamics [27-29], can promote the transcription of inflammatory signals and the direct activation of the NLRP3 inflammasome, leading to a further inflammatory response. Therefore, mitochon- dria are not only an important source of ROS in the inflammatory process, but also the target of ROS damage. This creates a feedback loop that regulate the body's inflammatory response. Our results showed that there was a significant inflammatory response and mitochondrial damage in human cardiomyocytes after radiation, which were mutually causal and jointly caused damage to cardiomyocytes. However, the specific regulatory mechanism still needs to be further explored.

What are the consequences of the cell damage caused by

the synergy of structure and functions? We found that microwave radiation can cause the apoptosis of cardiomyocytes, which is characterized by a significant increase in late apoptosis and decrease in viable cells, and the possible material basis are mitochondrial energy transfer disorders, ROS accumulation and elevated TNF-α expression. The established damage models of animals or cells caused by microwave radiation can only be compared when the parameters of band, frequency, and radiation time are consistent [9]. Human iPSC-CMs have begun to be introduced in this field because of their recent successful application in clinical patients with heart failure.

However, the effects of microwave radiation on hiPSC-CMs have not been well-documented. Given the potential clinical applications of hiPSC-CMs, it is important to understand how microwave radiation may influence their viability and function.

Author Statements

Author Contributions

Conceptualization, Y.-X.T., L.Y. and J.Z.; methodology, L.Y. and J.Z.; validation, L.Y., R.-L.M., Z.-M.Y., X.-P.X., P.-F.Z. and Q.L.; resources, R.-Y.P.; data curation, H.-T.C., B.-W.Y. and L.-M. F.; writing original draft preparation, L.Y. and J.Z.; writing—review and editing, Y.-X.T., C.-J.W. and R.-Y.P. All authors have read and agreed to the published version of the manuscript.

Conflicts of Interest

No potential competing interest was reported by the authors.

References

1. Sagar S, Adem SM, Struchen B, Loughran SP, Brunjes ME, Arangua L, et al. Comparison of radio frequency ectromagnetic field exposure levels in different everyday microenvironments in an international context. Environ Int. 2018; 114: 297-306.

2. Mercantepe T, Tümkaya L, Gökçe MF, Topal ZS, Esmer E. Effect of 900-MHz electromagnetic field on the cerebellum: A histopathological investigation. Sisli Etfal Hastan Tip Bul. 2018; 52: 129-34.

3. Stein Y, Udasin IG. Electromagnetic hypersensitivity (EHS, microwave syndrome) - Review of mechanisms. Environ Res. 2020; 186: 109445.

4. Zymantiene J, Juozaitiene V, Zelvyte R, Oberauskas V, Spancerniene U, Sederevicius A, et al. Effect of electromagnetic Field Exposure on Mouse Brain Morphological and Histopathological Profiling. J vet 297 res. 2020; 64: 319-24.

5. Leach V, Weller S, Redmayne M. A novel database of bio-effects from non-ionizing radiation. Rev Environ Health. 2018; 33: 273-80.

6. Tang J, Zhang Y, Yang L, Chen Q, Tan L, Zuo S, et al. Exposure to 900-MHz electromagnetic fields activates the mkp-1/ERK pathway and causes blood-brain barrier damage and cognitive impairment in rats. Brain Res. 2015; 1601: 92-101.

7. Vafaei S, Motejaded F, Ebrahimzadeh-Bideskan A. Protective effect of crocin on electromagnetic field-induced testicular damage and heat shock protein A2 expression in male BALB/c mice. Iran J Basic Med Sci. 2020; 23: 102-10.

8. Ruiz P, Gabarre P, Chenevier-Gobeaux C, François H, Kerneis M, Cidlowski JA, et al. Case report:changes in the levels of stress hormones during takotsubo syndrome. Front Cardiovasc Med. 2022; 9: 931054.

9. Zhang B, Zhang J, Yao BW, Xu XP, Wang H, Zhao L, et al. Dose-dependent, frequency-dependent, and cumulative effects on cardiomyocyte injury and autophagy of 2.856 GHz and 1.5-GHz microwave in Wistar rats. Biomed Environ Sci. 2022; 35: 351-5.

10. Li BL, Li W, Bi JQ, Zhao JG, Qu ZW, Lin C, et al. Effect of long-term pulsed electromagnetic field exposure on hepatic and immunologic functions of rats. Wien Klin Wochenschr. 2015; 127: 959-62.

11. Zhang J, Peng RY, Ren JH, Li J, Wang SM, Gao YB, et al. The protective effects of Aduola Fuzhenglin on the heart injury induced by microwave exposure in rats. Zhonghua Lao Dong Wei Sheng Zhi Ye Bing Za Zhi. 2011; 29: 367-70.

12. Wang H, Zhang J, Hu SH, Tan SZ, Zhang B, Zhou HM, et al. Real-time microwave exposure induces calcium efflux in primary hippocampal neurons and primary cardiomyocytes. Biomed Environ Sci. 2018; 31: 561-71.

13. Bekhite M, González-Delgado A, Hübner S, Haxhikadrija P, Kretzschmar T, Müller T, et al. The role of ceramide accumulation in human induced pluripotent stem cell-derived cardiomyocytes on mitochondrial oxidative stress and mitophagy. Free Radic Biol Med. 2021; 167: 66-80.

14. Zhang H, Xue Y, Pan T, Zhu X, Chong H, Xu C, et al. Epicardial injection of allogeneic human induced-pluripotent stem cell-derived cardiomyocytes in patients with advanced heart failure: protocol for a phase I/IIa dose-escalation clinical trial. BMJ Open. 2022; 12: e056264.

15. Lai YF, Wang HY, Peng RY. Establishment of injury models in studies of biological effects induced by microwave radiation. Mil Med Res. 2021; 8: 12.

16. Li D, Xu X, Gao Y, Wang J, Yin Y, Yao B, et al. Hsp72-based effect and mechanism of microwave radiation-induced cardiac injury in rats. Oxid Med Cell Longev. 2022; 2022: 7145415.

17. Yin Y, Xu X, Gao Y, Wang J, Yao B, Zhao L, et al. Abnormal expression of connexin43 in cardiac injury induced by S-band and X-band microwave exposure in rats. J Immunol Res. 2021; 2021: 3985697.

18. Zhu W, Cui Y, Feng X, Li Y, Zhang W, Xu J, et al. The apoptotic effect and the plausible mechanism of microwave radiation on rat myocardial cells. Can J Physiol Pharmacol. 2016; 94: 849-57.

19. Matsukawa A, Yoshimura T, Miyamoto K, Ohkawara S, Yoshinaga M. Analysis of the inflammatory cytokine network among TNF alpha, IL-1 beta, IL-1 receptor antagonist, and IL-8 in LPS-induced rabbit arthritis. Lab Invest. 1997; 76: 629-38.

20. Utsunomiya I, Ito M, Oh-ishi S. Generation of inflammatory cytokines in zymosan-induced pleurisy in rats: TNF induces IL-6 and cytokine-induced neutrophil chemoattractant (CINC) in vivo. Cytokine. 1998; 10: 956-63.

21. Mela L. Direct and indirect effects of endotoxin on mitochondrial function. Prog Clin Biol Res. 1981; 62: 15-21.

22. Su YW, Chiou WF, Chao SH, Lee MH, Chen CC, Tsai YC. Ligustilide prevents LPS-induced iNOS expression in RAW 264.7 macrophages by preventing ROS production and down-regulating the MAPK,NF-kappaB and AP-1 signaling pathways. Int Immunopharmacol. 2011; 11: 1166-72.

23. Cho KA, Suh JW, Lee KH, Kang JL, Woo SY. IL-17 and IL-22 enhance skin inflammation by stimulating the secretion of IL-1beta by keratinocytes via the ROS-NLRP3-caspase-1 pathway. Int Immunol. 2012; 24: 147-58.

24. Won JH, Park S, Hong S, Son S, Yu JW. Rotenone-induced impairment of mitochondrial electron transport chain confers a selective priming signal for NLRP3 inflammasome activation. J Biol Chem. 2015; 290: 27425-37.

25. Stiles L, Shirihai OS. Mitochondrial dynamics and morphology in beta-cells. Best Pract Res Clin Endocrinol Metab. 2012; 26: 725-38.

26. Nakahira K, Haspel JA, Rathinam VA, Lee SJ, Dolinay T, Lam HC, et al. Autophagy proteins regulate innate immune responses by inhibiting the release of mitochondrial DNA mediated by the NALP3 inflammasome. Nat Immunol. 2011; 12: 222-30.

27. Park J, Choi H, Min JS, Park SJ, Kim JH, Park HJ, et al. Mitochondrial dynamics modulate the expression of pro-inflammatory mediators in microglial cells. J Neurochem. 2013; 127: 221-32.

28. Ding S, Xu S, Ma Y, Liu G, Jang H, Fang J. Modulatory mechanisms of the NLRP3 Inflammasomes in diabetes. Biomolecules. 2019; 9.

29. Weiss-Sadan T, Maimoun D, Oelschlagel D, Kaschani F, Misiak D, Gaikwad H, et al. Cathepsins drive anti-inflammatory activity by regulating autophagy and mitochondrial dynamics in macrophage foam cells. Cell Physiol Biochem. 2019; 53: 550-72.